

Meshing of a Spiral Bevel Gear Set With 3-D Finite Element Analysis

George D. Bibel & Robert Handschuh

Abstract

Recent advances in spiral bevel gear geometry and finite element technology make it practical to conduct a structural analysis and analytically roll the gear set through mesh. With the advent of user-specific programming linked to 3-D solid modelers and mesh generators, model generation has become greatly automated. Contact algorithms available in general purpose finite element codes eliminate the need for the use and alignment of gap elements. Once the gear set is placed in mesh, user subroutines attached to the FE code easily roll it through mesh. The method is described in detail. Preliminary results for a gear set segment showing the progression of the contact line load is given as the gears roll through mesh.

Introduction

One of the most complex and highly loaded components in a helicopter is the main rotor transmission (Cormier, 1979). One of the critical components of the transmission is the spiral bevel gear mesh.

The designer is faced with tradeoffs between weight and reliability. Weight reduction results in increased flexibility and deflection of the teeth and rim. Deflection of the gear creates a departure from the expected contact found by rolling the gears. These deflections cause the contact zone to shift. The shift in contact can dramatically increase contact and tooth bending stresses with a corresponding reduction of component life.

The contact ellipse and localized stress distribution have been historically analyzed with Hertzian theory developed for ball and roller bearing elements (Coy et al., 1985). This theory considers the contact stresses for two general surfaces with direct bearing load. Gear teeth are not loaded directly. The load is transmitted through flexible teeth connected to flexible rims. The tooth and rim flexing of the gear and pinion will greatly affect the location and shape of the contact zone, load sharing between teeth and the contact stress distribution. These factors will in turn affect fatigue life, noise and vibration, thermal degradation and hydrodynamic action of the lubricant. These issues are also important design parameters for spiral bevel gearing in ground vehicles.

Considerable work has been completed to automate 3-D modeling of spiral bevel gears. Fundamental to this work is an understanding of the gear surface geometry. Litvin (1989) and Litvin & Tsung (1989) presented the theory of spiral bevel gear generation and design. Handschuh and Litvin (1991) extended this analysis to the mathematical description of the gear tooth surfaces.

Bibel et al. (1993, 1994) began the automation of the analysis with model development software that creates input for the 3-D solid modeler

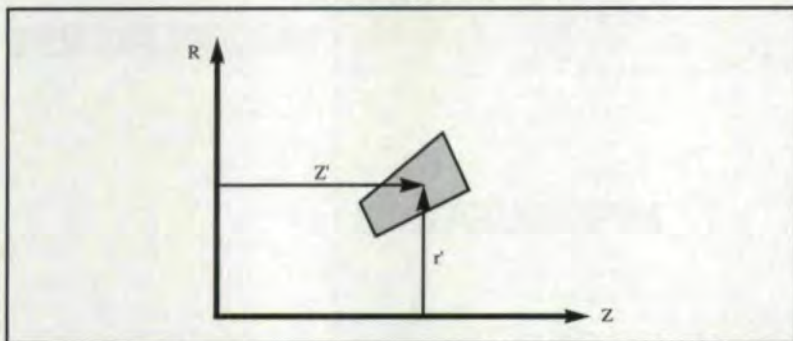


Fig. 1 — Axial and radial projections of gear surface into RZ plane.

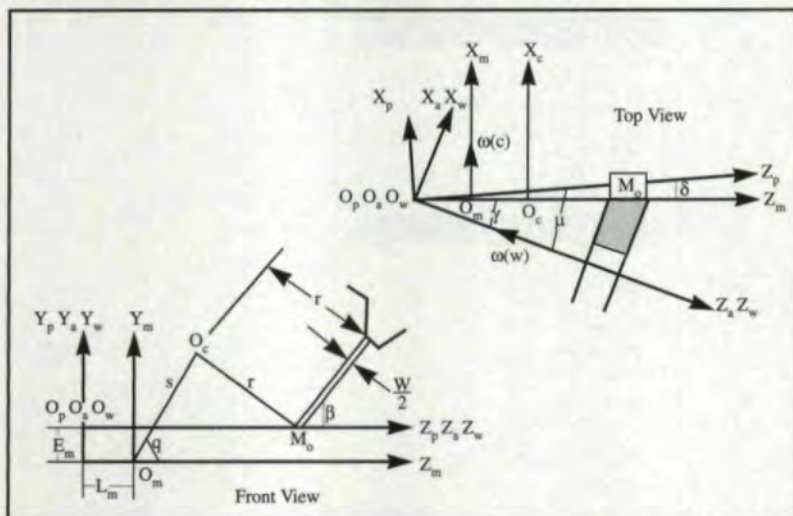


Fig. 2 — Coordinate system orientation to generate a right-hand gear surface ($\phi_c = 0$ shown here).

(PATRAN) and the finite element code NAS-TRAN. The finite element modeling done with NASTRAN utilized gap elements. The analysis was greatly simplified by using the contact algorithm in the finite element code MARC (Bibel et al. 1994). A user subroutine compiled with the MARC input file rotates the gear set through mesh.

This work is being extended into a series of programs that receive machine tool settings as input and create 3-D contact analysis of spiral bevel gears rolling through mesh.

Surface Geometry

The most difficult task associated with 3-D modeling of spiral bevel gears in mesh is an accurate description of the gear surface geometry. The surface of a generated gear is an envelope to the family of surfaces of the head cutter. In other words, the points on the generated tooth surface are points of tangency to the cutter surface during manufacture.

The conditions necessary for envelope existence are given kinematically by the equation of meshing. The equation is stated as follows: The normal of the generating surface must be perpendicular to the relative velocity between the cutter and the gear tooth surface. This is given mathematically as

$$\mathbf{n} \cdot \mathbf{V} = 0$$

where \mathbf{n} is the normal vector and \mathbf{V} is the relative velocity.

The equation of meshing for straight-sided cutters with a constant ratio of roll between the cutter and workpiece is given in Litvin et al. (1989 and 1991) as

$$(u - r \cot \psi \cos \psi) \cos \gamma \sin \tau + s[(m_{cw} - \sin \gamma) \cos \psi \sin \theta \mp \cos \gamma \sin \psi (q - \phi_c)] \mp E_m (\cos \gamma \sin \psi + \sin \gamma \cos \psi \cos \tau) - L_m \sin \gamma \cos \psi \sin \tau = 0 \quad \text{Eq. 1}$$

where $\tau = (\theta \mp q \pm \phi_c)$

γ = the root angle of the component being manufactured.

u, θ locate a point on the cutting head as given in Handschuh et al., 1991.

ϕ_c = the cradle orientation.

ψ = the blade angle.

r = the radius of the cutter.

L_m = the vector sum, a machine tool setting described in Handschuh et al., 1991.

E_m = machine offset, a machine tool setting described in Handschuh et al., 1991.

s = cradle to cutter distance.

q = cradle angle.

m_c = ratio of angular velocity of the cradle to the workpiece.

All of the above terms, except u, θ and ϕ_c , are known machine tool settings for a given gear set

design. These three terms can be numerically solved for if two additional equations are identified.

The points on the gear surfaces found by solving the equation of meshing must also satisfy the axial and radial location of a projection into the RZ plane that identifies the generated workpiece.

This is satisfied by the following:

$$Z_w - Z' = 0 \quad \text{Eq. 2}$$

$$r' - (X_w^2 + Y_w^2)0.5 = 0 \quad \text{Eq. 3}$$

where X_w, Y_w and Z_w are coordinates of a point on the workpiece in the workpiece coordinate system, and Z' and r' are the axial and radial projections into the RZ plane of the workpiece as shown in Fig. 1.

Equations 1, 2 and 3 can be solved with a numerical iterative procedure. Equation 1 is given in terms of cutting head coordinates u, θ and ϕ_c , whereas Equations 2 and 3 are given in terms of workpiece coordinates X_w, Y_w and Z_w .

A point on the head cutter \mathbf{r}_c (written in terms of u, θ and ϕ_c) must be transformed into a point on the workpiece \mathbf{r}_w (written in terms of X_w, Y_w and Z_w with the following series of homogeneous coordinate transformations.

$$\mathbf{r}_w = [\mathbf{M}_{wa}][\mathbf{M}_{ap}][\mathbf{M}_{pm}][\mathbf{M}_{ms}][\mathbf{M}_{sc}]\mathbf{r}_c \quad \text{Eq. 4}$$

where $[\mathbf{M}_{wa}]$, $[\mathbf{M}_{ap}]$, $[\mathbf{M}_{pm}]$, $[\mathbf{M}_{ms}]$ and $[\mathbf{M}_{sc}]$ are a series of matrix coordinate transformations given in Litvin, 1989, Litvin et al., 1989 and Handschuh et al., 1991.

These coordinate systems are described as follows and shown in Fig. 2 for a right-hand gear surface. The head-cutter coordinate system S_c is rigidly connected to the cradle coordinate systems S_s . S_s rotates about fixed coordinate system S_m attached to the machine frame. Coordinate system S_p orients the pitch apex of the gear being manufactured. The common origin for coordinate systems S_p and S_a locates the apex of the gear under consideration with respect to system S_m . The final transformation is from coordinate system S_a to S_w , which is fixed to the component being manufactured.

A computer program was written using the above solution technique. This program receives machine tool settings and basic gear geometry as input and creates an output file containing the coordinates of surface points for the gear and pinion. The output from this program is read by a second computer program. This program uses the surface points as input and creates an output file that can be compiled and read into the 3-D solid modeler PATRAN (1991). PATRAN is used to create a NASTRAN or MARC input deck of any mesh density.

A gear set model created in this manner is shown in Fig. 3. The description of these two programs and coding is given in Bibel et al. (1993 and 1994).



Fig. 3 — Spiral bevel gear set modeled as described in text.

Dr. George D. Bibel

is Associate Professor of Mechanical Engineering at the University of North Dakota, Grand Forks, ND.

Dr. Robert Handschuh

is with the Vehicle Technology Directorate, U.S. Army Research Laboratory, NASA Lewis Research Center, Cleveland, OH.

Gap Elements

Previously 3-D contact analysis was accomplished using gap elements. This presented numerous problems related to gap element orientation. After the contact point was located, the surface normal at the contact point was calculated. Lines parallel to the contact point surface normal were constructed from nodes on the pinion.

The intersection of these lines with the gear surface was then calculated. These intersection points on the gear's surface were then incorporated into new, distorted elements on the gear. For

every new gear surface node that was added, an existing gear surface node had to be deleted, and the element nodal connectivity had to be redefined. For coarse models, it worked reasonably well to select the new element connectivity by visual inspection. Larger models would require calculation of various permutations of nodal connectivity and distances to determine the most appropriate nodal substitutions and new element connectivity. The resulting remapped elements on the gear surface are shown in Fig. 4.

However, to roll the gear set through mesh, the entire process of contact point and contact point surface normal calculation, intersection of lines from pinion nodal points with a gear surface, definition of new element connectivity on gear surface and calculation of gaps had to be repeated for every incremental rotation. Typical output from a gap element model is shown in Fig. 5. Although the model was relatively coarse, the results compared favorably with Hertzian estimates.

Contact Algorithm

Greatly superior to the method of gap elements is the automated contact algorithm described in MARC K-5.1 (1991). Contact between deformable bodies is handled by imposing non-penetrating constraints as shown in Fig. 6. Automatic in this context means that user interaction is not required in treating multi-body contact. The program has automated the imposition of non-penetration constraints, even while rolling through mesh. The user no longer has to worry about the location, orientation and open/close status checks of "gap elements." Typical output for contact analysis from the contact algorithm is shown in Fig. 7. The results were consistent with previous modeling done with gap elements and with Hertzian estimates.

Automated Meshing With User Subroutine

The model development software mathematically creates the pinion and gear surface coordinates along the same axis of rotation. The gear and pinion must be properly located for meshing action. First the pinion is rotated a small angle about its axis of rotation to accommodate tooth mesh alignment.

The pinion is placed in mesh by a rotation θ corresponding to the shaft angle. The gear set is now properly positioned for 3-D contact analysis with MARC.

After completion of an increment of the finite element contact analysis with MARC, the gear and pinion are rotated by a user subroutine to simulate the gears rolling through mesh. For meshing, the gear is rotated a small increment of " δ " degrees. The pinion would then rotate " $\delta \cdot$

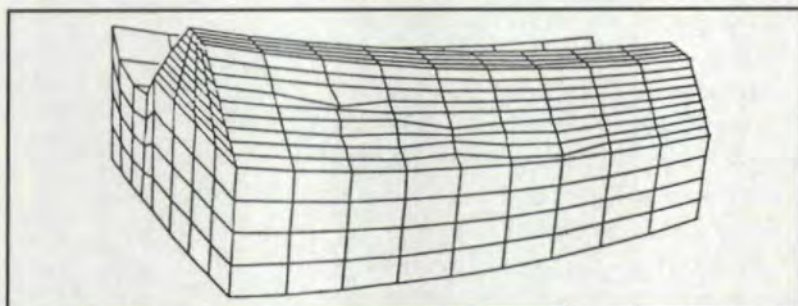


Fig. 4 — Distorted gear surface FE mesh required for gap element orientation.

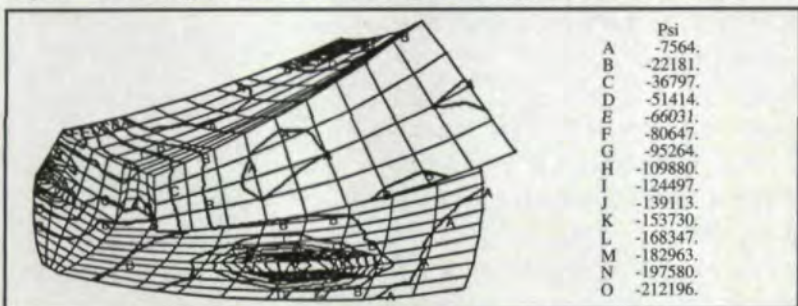


Fig. 5 — Typical contact stress contours from gap element model.

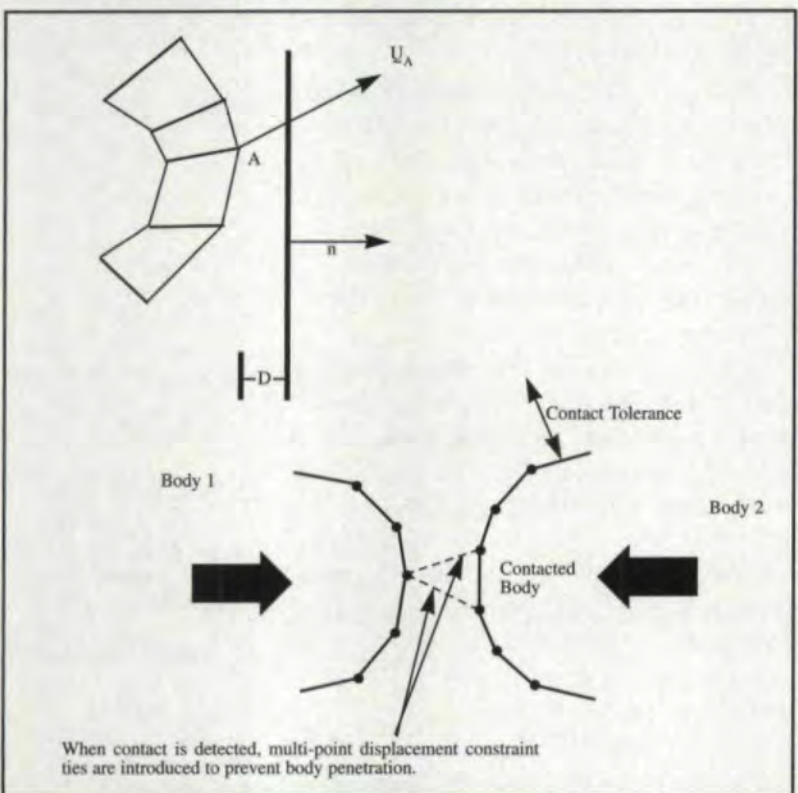


Fig. 6 — Non-penetrating constraints used in contact algorithm.

(Number of Gear Teeth)/(Number of Pinion Teeth)" in the opposite sense. The finite element contact analysis is repeated for a new orientation of the gear set. The process is repeated by merely changing the two numbers corresponding to the rotations of the gear set in the user subroutine.

The user subroutine is written in FORTRAN and compiles with the MARC input file.

Preliminary Results

A two-tooth pinion segment and a two-tooth gear segment were rolled through mesh with increments of about one degree of pinion rotation. (There are 19 teeth on the pinion.)

A series of plots is shown in Fig. 8. Shown is a plot of line loading of the forces on the pinion as it rolls through mesh in a counterclockwise direction. The line load is seen to progress from the heel of the back pinion tooth to the toe.


The loading switches from the back pinion tooth to the front after a brief period of load sharing. Also shown is an example of line loading on the gear for a single configuration in Fig. 9.

More work remains to be done concerning mesh refinement, enhanced accuracy of the modeling of the fillet region, better boundary conditions, etc. The work at this point is considered analogous to initial attempts at 2-D FE modeling of spur gears. The models went through a natural progression of increased complexity (i.e., single-tooth models with point contact, multi-tooth models with point contact, multi-tooth models with deformable contact, etc.) As computers became more powerful and the technology became more mature, eventually entire planetary gear sets were rolled through mesh with 2-D models. 3-D modeling needs to go through a similar evolution.

Conclusion

Considerable progress has been made in automating 3-D analysis of spiral bevel gears in mesh. Programs have been written that start with machine tool settings and can create finite element models of any mesh density. This is done by numerically evaluating the kinematic motion of the manufacturing process for generated spiral bevel gears and creating input data for a commercially available 3-D solid modeler.

Deformable gear tooth contact is modeled with the automatic generation of non-penetration constraints. This is done by contact algorithm in a commercially available finite element code. The contact algorithm eliminates the problems of mesh distortion associated with calculating the location and orientation of gap elements.

Although the original finite element analysis was done on a supercomputer, the software used is now available on a desktop PC. 

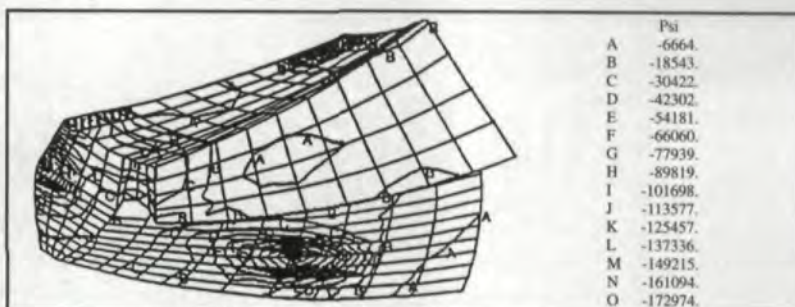


Fig. 7 — Typical contact stress contours from contact algorithm FE model.

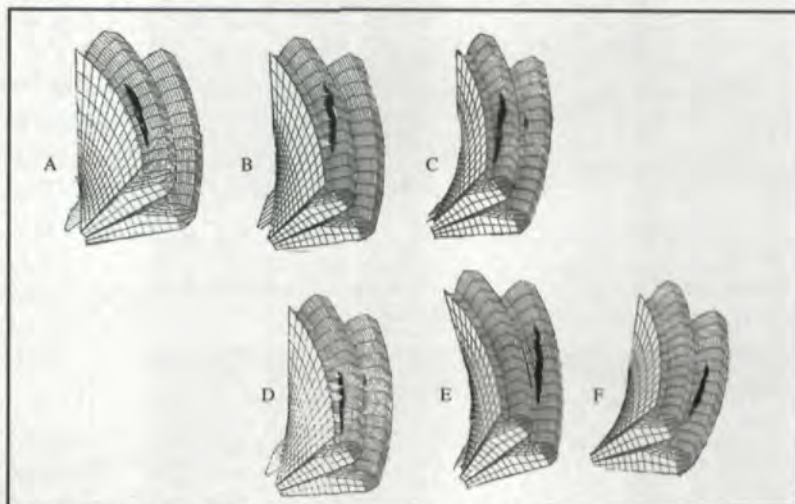


Fig. 8 — Plot of contact forces for pinion segment rolling through mesh.

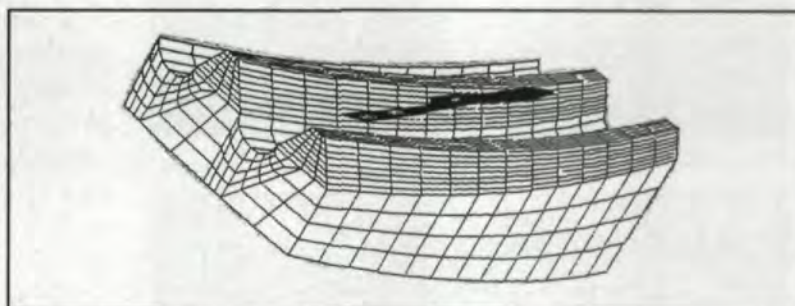


Fig. 9 — Typical plot of contact forces on two-tooth gear segment.

References:

1. Bibel, G. D. et al. "Contact Stress Analysis of Spiral Bevel Gears Using Nonlinear Finite Element Static Analysis." NASA Technical Memorandum 106176 AIAA-93-2296 ARL-TR-158, May 1993.
2. Bibel, G. D. et al. "Manual for Automatic Generation of Finite Element Models of Spiral Bevel Gears in Mesh." NASA Contractor Report 191009, Army Research Laboratory Report ARL-CR-121, April, 1994.
3. Bibel, G. D. et al. "Prediction of Contact Path and Load Sharing in Spiral Bevel Gears." NASA Contractor Report 195305, Army Research Laboratory Report ARL-CR-146, April, 1994.
4. Bibel, G. D. et al. "Comparison of Gap Elements and Contact Algorithm for 3-D Contact Analysis of Spiral Bevel Gears." NASA Technical Memorandum 106643, Army Research Laboratory Technical Report ARL-TR-478, 1994.
5. Cormier, K. R. "Helicopter Drive System Reliability and Maintainability Design Guide." USARTL-TR-78-50, April, 1979.
6. Coy, J. J. et al. "Gearing." NASA Reference Publication 1152, December, 1985.
7. Handschuh R. F. & Litvin, F. L. "A Method for Determining Spiral Bevel Gear Tooth Geometry for Finite Element Analysis." NASA Technical Paper 3096 AVSCOM Technical Report 91-C-020, August, 1991.
8. Handschuh, R. F. & Kicher, T. P. "Method for Thermal Analysis of Spiral Bevel Gears." NASA Technical Memorandum 106612 ARL-TR-457, July, 1994.
9. Litvin, F. L. *Theory of Gearing*. AVSCOM Technical Report 88-C-035, 1989.
10. Litvin, F. L. & Tsung, W. "Generation of Spiral Bevel Gears with Conjugate Tooth Surfaces and Tooth Contact Analysis." AVSCOM Technical Report 87-C-22, 1989.
11. Litvin, F. L. et al. "Users Manual for Tooth Contact Analysis of Face-Milled Spiral Bevel Gears With Given Machine-Tool Settings." NASA Contractor Report 189093, AVSCOM Technical Report 91-C-051, December 1991.
12. *MARC K-5.1 User Manual*. MARC Analysis Research Corporation, Palo Alto, CA, 1991.
13. *PATRAN Users Manual*. PDA Engineering, Costa Mesa, CA, 1991.

Tell Us What You Think . . .

If you found this article of interest and/or useful, please circle 206.